225-GHz atmospheric opacity of the South Pole sky derived from continual radiometric measurements of the sky-brightness temperature

Richard A. Chamberlin and John Bally

We report measurements of the atmospheric opacity of the South Pole at 225 GHz for the period from day 3 to day 180 in 1992. These opacity data were derived from continual radiometric measurements of the sky-brightness temperature as a function of the zenith angle. These radiometric measurements were performed with a 225-GHz heterodyne atmospheric radiometer on loan from the National Radio Astronomy Observatory. This radiometer was previously used to characterize other candidate millimeter and submillimeter radio-telescope sites. We found that the atmospheric opacity was below 0.098 air mass^{-1} 75% of the time from day 3 to day 70 in 1992, and below 0.055 air mass^{-1} 75% of the time from day 70 to day 180 in 1992. Thus, our data demonstrate that the South Pole is an excellent site for performing millimeter- and submillimeter-wavelength radio astronomy.

Key words: 225-GHz atmospheric opacity, South Pole, telescope site selection.

1. Introduction

Previous measurements of the South Pole sky using radiometric techniques[1] and analysis of upper-air data[2] indicate that the South Pole is an excellent site for performing ground-based astronomical observations in the infrared-, millimeter-, and submillimeter-wavelength regimes. The characteristics that make the South Pole an excellent site are its physical elevation (3,000 m) combined with a very low column density of atmospheric water vapor. These factors make the sky there very transparent at wavelengths where water-vapor radiative emission and absorption are significant. We present here a continual record of the South Pole's atmospheric opacity at 225 GHz from day 3 to day 180 of the year 1992. These data were derived from continual zenith-to-horizon measurements of the atmospheric sky-brightness temperature. These measurements where made with a 225-GHz heterodyne radiometer on loan from the National Radio Astronomy Observatory (NRAO). This type of radiometer has previously been used to characterize the opacity at other sites, such as Mauna Kea.[3]

2. Apparatus and Method

The NRAO 225-GHz atmospheric radiometer that we used is described elsewhere,[4,5] so we provide only a short description here. The radiometer is a superheterodyne receiver employing a Schottky diode mixer that is temperature stabilized to 45 °C. The radiometer is calibrated by measurement of two internal blackbody reference loads that are temperature stabilized to the nominal values of 45 °C and 65 °C. The input beam to the mixer is switched between the two reference loads and the sky source by a four-bladed chopper turning continuously at 2.5 rps. The zenith angle z of the sky source imaged onto the mixer is directed by a steerable mirror. The steerable mirror is attached to a stepper motor that can turn in 1.8° steps under computer control. The steerable mirror and the stepper motor are external to the instrument enclosure and the beam from the mirror is focused into the enclosure through a thin Mylar window. The half-power beam width of the optical system is approximately 4°. The steerable mirror had a small hole drilled into its center for mechanical-alignment purposes. To reduce unwanted beam diffraction, we affixed a small piece of reflective Mylar tape over the hole. The local oscillator for the mixer is supplied

The authors are with the Center for Astrophysical Research in Antarctica, Yerkes Observatory, Williams Bay, Wisconsin 53191. R. A. Chamberlin is also with the Department of Astronomy, Boston University, 725 Commonwealth Avenue, Boston, Massachusetts 02215; and J. Bally is with the Department of Astrophysical, Planetary, and Atmospheric Sciences, Campus Box 391, and the Center for Astrophysics and Space Astronomy, Campus Box 389, University of Colorado, Boulder, Colorado 80309.

Received 9 November 1992; revision received 25 August 1993.
0003-6935/94/061095-05$06.00/0.

from a frequency-tripled Gunn oscillator operating at 75 GHz and temperature stabilized to 45 °C. The intermediate-frequency (IF) output from the mixer is amplified and filtered with a filter having a bandpass of 1 to 2 GHz; thus, the IF-center frequency is 1.5 GHz, with a detection bandwidth of 1 GHz. The IF power is detected with a square-law detection circuit whose output is presented to three sample-and-hold circuits, which are synchronized with the phase of the chopper. The outputs of the three sample-and-hold circuits are presented to two differential amplifiers that produce voltage levels proportional to $(W_{sky} - W_{ref})$, and $(W_{hot} - W_{ref})$, where W_{sky} represents the total power detected by the radiometer from the sky source, W_{ref} represents the total power detected by the radiometer from the 45 °C reference load, and W_{hot} represents the total power detected by the radiometer from the 65 °C reference load. The three voltage levels $(W_{sky} - W_{ref})$, $(W_{hot} - W_{ref})$, and W_{ref} are presented to an analog-to-digital converter that can be continually read by an external computer over a serial interface. The system temperature of the radiometer was found to be approximately 2050 K.

The NRAO radiometer was originally designed to operate at a minimum temperature of −20 °C. To enable it to operate at the South Pole, where the minimum temperature can reach −80 °C, the instrument enclosure was covered with both a temperature-controlled heating foil (Minco Models HK5184R26.4L12B and CT137PD), and a 1.5-in-thick layer of styrofoam insulation epoxyed on top of the heating foil. The heating-foil system could produce up to 300 W if required, and the foil-temperature controller was set to keep the enclosure temperature stable to 10 °C. The instrument's steerable mirror and Mylar window were periodically checked for frost and snow accumulation and cleaned by a technician on site at the South Pole.

The radiometer was interfaced to a multitasking, multi-user computer (i486, running LynxOS) by means of a serial interface built in to the radiometer. A program was run on the computer to change the zenith angle of the steerable mirror, record the computer clock time, and acquire the values $(W_{sky} - W_{ref})$, $(W_{hot} - W_{ref})$, W_{ref}, T_{ref}, T_{hot}, and T_{surf}, where T_{ref} is the actual temperature of the nominal 45 °C blackbody-reference load, and T_{hot} is the actual temperature of the nominal 65 °C blackbody-reference load. T_{surf} is the outside surface air temperature measured by an electronic thermometer on the outside of the radiometer enclosure. The computer was programmed to make two zenith-to-horizon scans with the steerable mirror approximately every 45 min. Each scan sampled 22 different zenith angles. After each steerable mirror movement, the computer was programmed to wait 10 sec before acquiring any new data, to allow the low-pass filters on the inputs of the chopper-synchronized sample-and-hold circuits to completely decay to their new voltages. Following this waiting period, the measurement interval at each sampled angle was approximately 10 sec, during which time the radiometer serial interface was read by the computer 20 times and the acquired values averaged. Each scan lasted approximately 8 min and sampled the following zenith angles: 0°, 9.0°, 18.0°, 27.0°, 30.6°, 36.0°, 41.4°, 45.0°, 48.6°, 54.0°, 59.4°, 64.8°, 70.2°, 75.6°, 77.4°, 79.2°, 81.0°, 82.8°, 84.6°, 86.4°, 88.2°, 90.0°. The three largest zenith angles were not used in any analyses because of possible beam contamination from ground spill-over. As described below, we did not find any effect from beam spill-over up to the zenith angle of 84.6°.

Each day, a data file of the previous day's measurements was created and transmitted by satellite from the South Pole to a local computer in North America. The data were reduced as follows: The sky brightness temperature at zenith angle z was calculated from

$$T_{sky}(z) = (W_{sky} - W_{ref})^*(T_{hot} - T_{ref}) /(W_{hot} - W_{ref}) + T_{ref} + 273.16, \quad (1)$$

with $T_{sky}(z)$ expressed in Kelvins. The sky-brightness temperatures were then used to determine the atmospheric opacity, with a slab model for the atmosphere:

$$T_{sky}(z) = T_0 + T_{at}\{1 - \exp[-\tau A(z)]\}, \quad (2)$$

where $T_{sky}(z)$ is the radiometric temperature of the sky at zenith angle z; T_0 is the static background radiation detected by the radiometer because of primary mirror and Mylar window emissivity, and beam spillover; τ is the opacity; and $A(z)$ is the optical path length through the atmosphere corresponding to zenith angle z. The optical path length at the zenith, $A(z = 0)$, is defined as one air mass. T_{at} is an average of the atmospheric temperature in the column of air measured by the radiometer. In Eq. (2) we neglected to include any contribution from the cosmic microwave background radiation because the brightness temperature of this radiation at 225 GHz is only approximately 0.2 K. [Equation (2) can be derived from a differential form of the Beer–Lambert law, which is modified to include a source term for atmospheric thermal radiation. Integration, application of the appropriate boundary conditions, and expression of radiation intensities in terms of brightness temperatures gives the second term in Eq. (2)]. For a plane-parallel atmosphere, $A(z)$ can be approximated by $1/\cos(z)$, but we calculated $A(z)$ from

$$A(z) = -0.0045 + 1.00672/\cos(z) - 0.002234 /[\cos(z)]^2 - 0.0006247/[\cos(z)]^3, \quad (3)$$

which corrects $A(z)$ for the Earth's curvature.[6]

The values T_0, T_{at}, and τ can be derived from the fit of Eq. (2) to the plot of $T_{sky}(z)$ versus $A(z)$. However, to improve the stability of the fit by reducing the number of free-fit parameters, T_{at} was made to be equal to the surface ambient temperature, T_{surf}, measured at the radiometer. This should be a reason-

ably good approximation because: first, water vapor is most abundant near the surface; and second, water-vapor attenuation at 225 GHz is mainly caused by pressure broadening of the emission lines, which is most significant near the surface.[7] Previous workers used a value of T_{at}, which was approximately 95% of the surface temperature[5] because they assumed an adiabatic lapse rate of 9.8 K/km. At the South Pole, an inversion layer is usually present, so we assumed that $T_{at} = T_{surf}$ for our analysis. However, the derived values of opacity are not too sensitive to the values of T_{at}. For example, inspection of Eq. (2) shows that an error of 5% in the estimation of T_{at} results in an error of nearly 5% in the estimation of τ for a low-opacity sky. An error in the opacity of this magnitude would not affect our general conclusions about the merits of the South Pole sky.

3. Results and Discussion

Figure 1 shows the surface atmospheric temperature T_{surf} versus the number of elapsed days from the beginning of 1992. Some data in this period is not available because the radiometer was out of service for maintenance. Figure 2 is a plot of $T_{sky}(z)$ versus $A(z)$ from a typical radiometer scan. The solid points are the values of $T_{sky}(z)$ measured from zenith to 84.6°, (9.6 air masses). These data were taken on day 122 (1 May 1992, 0006 UT). The result of the fit of Eq. (2) to these data is shown as a curve. As described above, T_{at} was taken to be equal to the surface temperature, which was 217.5 K. The fit of Eq. (2) to the data gives the values $\tau = (0.056 \pm 0.001)$ air mass^{-1}, and $T_0 = 44.4$ K. Because of the possibility of beam contamination from ground spill-over at the larger zenith angles, we also analyzed the data presented in Fig. 2 by cutting off the curve fit at a zenith angle of only 70.2° at 2.9 air masses. In this later case we found that $\tau = (0.055 \pm 0.003)$ air mass^{-1}, which indicates that beam contamination from ground spill-over is not a significant effect even at the rather large zenith angle of 84.6°. The somewhat high value of T_0 is almost entirely due to thermal emission from the Mylar window in the enclosure. The original Mylar window was much thinner and produced much less thermal emission. However, this window broke and was replaced with the thicker on day 90 (30 March 1992).

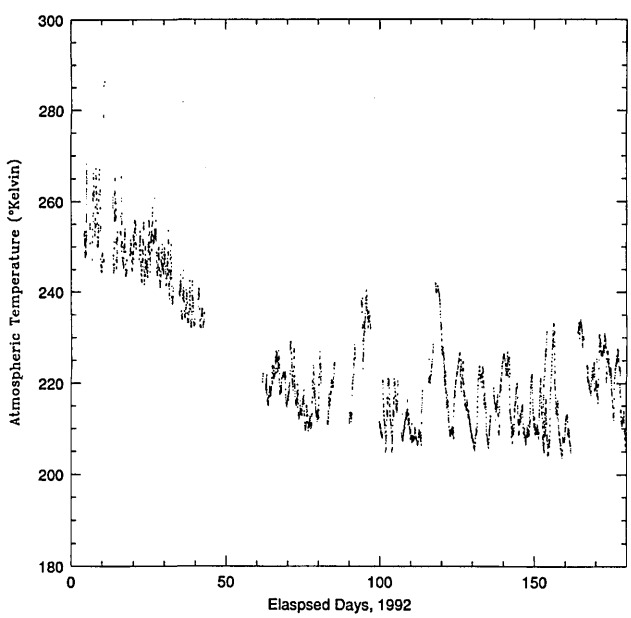

Fig. 1. The points shown are the surface temperatures measured by an electronic thermometer on the NRAO radiometer.

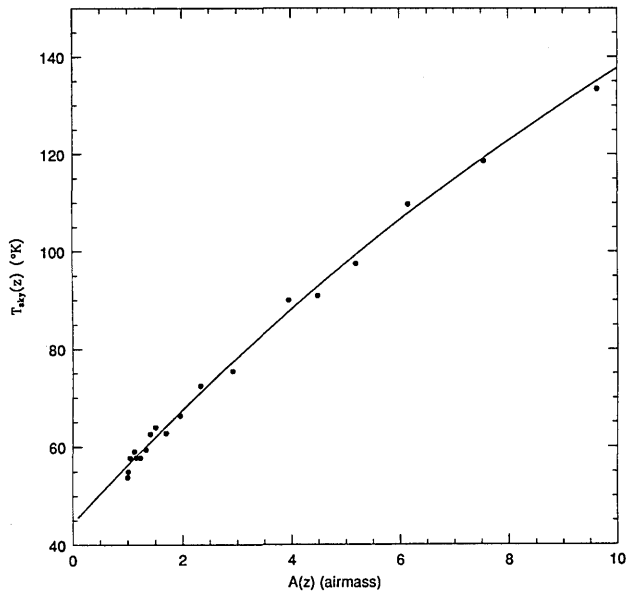

Fig. 2. This graph shows the results of a typical zenith-to-horizon sky-brightness measurement scan. The solid points are radiometric measurements of the sky-brightness temperature. The line is a fit of the Eq. (2) to these data. According to this fit, $\tau = 0.056$ air mass^{-1}, and $T_0 = 44.4$ K, with $T_{at} \equiv 217.5$ K. The standard deviation of the averaged measurements for each point was less than 0.5 K; therefore, no error bars are shown.

Figure 3 is a plot of the deduced opacities versus elapsed days from day 3 to day 180 in 1992. The big gap in the data from day 42 to day 61 was due to a computer-operating-system problem that stopped data acquisition during this period. The smaller gaps in the Fig. 3 are due to data transmission not being received or to the radiometer being out of service for maintenance. Inspection of Fig. 3 shows that the data can be roughly divided into two periods. The first period, day 3 to day 70, corresponds to the Austral summer, and it is a period of higher opacities: 0.04–0.20 air mass^{-1}. The second period, day 70 to day 180, corresponds to the Austral winter, and it is a period of consistently low opacities: 0.03–0.07 air mass^{-1}.

Figure 4 is a plot of the percent of observations for which τ was below a given value for the period from day 3 to day 70. Because the τ observations were spaced at equal intervals in time, Fig. 4 would be representative of the percent of time one could have expected τ to be below the given value. The quartiles in Fig. 4 are 0.068, 0.080, 0.098, and 0.177, i.e., the opacity was 0.068 or less 25% of the time; 0.080 or

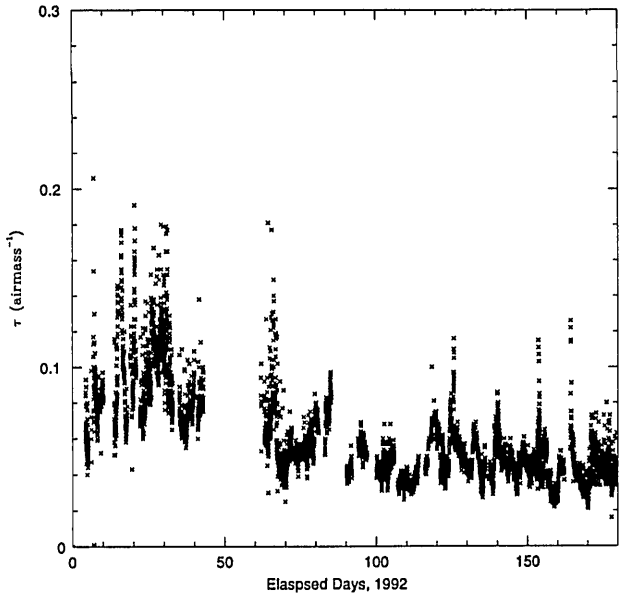

Fig. 3. The deduced atmospheric opacity τ versus elapsed days in 1992.

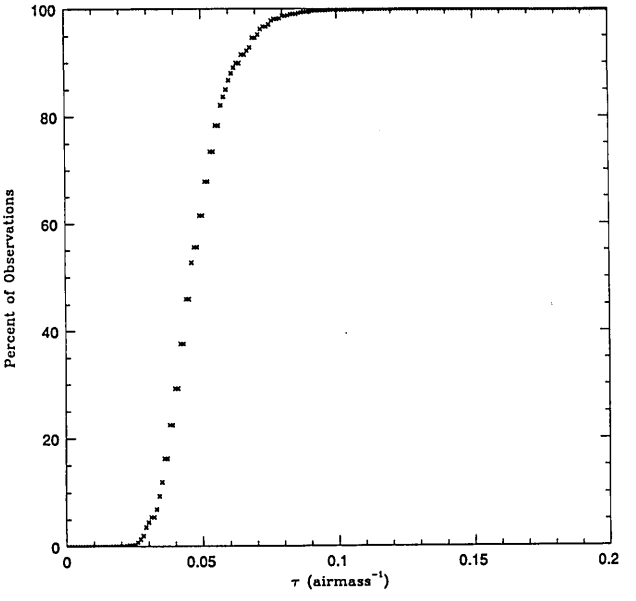

Fig. 5. The percent of observations for which τ was less than a given value for the period of day 70 to day 180.

less 50% of the time; 0.098 or less 75% of the time; and 0.177 or less 99.5% of the time. Figure 5 is a corresponding graph of the percent of observations for which τ was below a given value for the period from day 70 to day 180. The quartiles in Fig. 5 are 0.039, 0.046, 0.055, and 0.090. These quartile data are also presented in Table 1.

The above quartile data were obtained by fitting Eq. (2) to the dependence of T_{sky} on $A(z)$ up to $A(z) =$ 9.6 air masses ($z = 84.6°$). To check if the inclusion of the largest zenith angles was somehow biasing our resulting quartile data, we reanalyzed all of the data, limiting $A(z)$ to a maximum value of 2.9 air masses ($z = 70.2°$). This cutoff of the analysis at 2.9 air masses corresponds with the method of earlier workers.[5] Accordingly, the reanalysis produced the following quartiles: day 3 to day 70: 0.061, 0.075, 0.093, and 0.190; and day 70 to day 180: 0.039, 0.047, 0.058, and 0.110. These data are also presented in Table 1. From the previous discussion about the data in Fig. 2 and the quartile data in Table 1, we can see no large systematic difference between data analyzed with $A(z)$ cut off at 2.9 air masses, and $A(z)$ cut off at 9.6 air masses.

A similar NRAO 225-GHz radiometer was used to deduce the opacities of the sky at Mauna Kea by other workers. Their data show[3] the very best three-month period at Mauna Kea (1 April 1991 to 30 June 1991) had opacity quartiles of 0.046, 0.069, and 0.121. The 100% opacity quartile is not reported, but it would have been greater than 0.5. The worst three-month period reported at Mauna Kea (1 October 1989 to 31 December 1989) had opacity quartiles of 0.064,

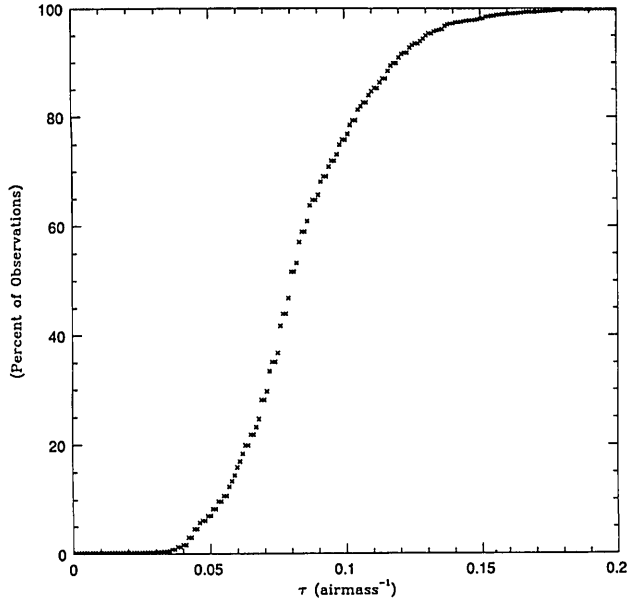

Fig. 4. The percent of observations for which τ was less than a given value for the period of day 3 to day 70.

Table 1. 225-GHz Opacity Quartiles for the South Pole and Mauna Kea[a]

Max. $A(z)$ used in analysis	South Pole[b]				Mauna Kea	
	9.6 Air Masses		2.9 Air Masses		2.9 Air Masses	
	Summer	Winter	Summer	Winter	Worst	Best
Quartile						
25%	0.068	0.039	0.061	0.039	0.064	0.046
50%	0.080	0.046	0.075	0.047	0.140	0.069
75%	0.098	0.055	0.093	0.058	0.263	0.121
99.5%	0.177	0.090	0.190	0.110	not reported (>0.5)	

[a]Summer and winter, best and worst reported quartiles. See text and Ref. 3 for details of the Mauna Kea measurement periods. South Pole measurements taken in 1992.

[b]South Pole quartile results are shown for two cases of data analysis: with the fit of Eq. (2) cut off at 9.6 air masses and with the fit cut off at 2.9 air masses.

0.140, and 0.263, with the 100% quartile not reported. The entire measurement period at Mauna Kea extended from 1 September 1989 to 31 August 1991. These data are also presented in Table 1 for the purpose of comparison. The details of the methods of data acquisition and analysis are different between the work presented here and the previously reported Mauna Kea work, and it is possible that, although the radiometers are identical by design, they may differ in operation. However, we know of no significant bias caused by differing methods or instrumentation that would prevent comparison of the general results from the two sites. In fact, our experience indicates that the opacity values derived from sky-brightness measurements made with the NRAO 225-GHz radiometer are relatively insensitive to the details of the data-acquisition and data-reduction methods.

4. Conclusions

At the present time, Mauna Kea is considered to be a premier site for performing ground-based millimeter and submillimeter radio astronomy. Our data show that South Pole summertime opacities at 225 GHz are comparable to those found at Mauna Kea at the 25% quartile level. However, the opacity data presented in Table 1 do show that the summertime observing conditions at the South Pole were favorable a greater percentage of the time, particularly at the 75% and 100% quartile levels. Wintertime observing conditions were favorable at all quartile levels when compared with the best data reported from Mauna Kea (see Table 1). Therefore, the opacity data reported here strongly recommend the South Pole as a site for performing year-round millimeter and submillimeter radio astronomy.

This work was partially supported by National Science Foundation grant NSF DPP 89-20223 to the Center for Astrophysics Research in Antarctica (CARA). CARA is a National Science Foundation Science and Technology Center. The 225-GHz radiometer we used was generously loaned to us by the National Radio Astronomy Observatory. Our data-acquisition computer was loaned to us by the Radio Physics Department of AT&T Bell Laboratories, Crawford Hill, New Jersey. We thank D. Ledoux, the South Pole winterover technhician, for his efforts on our behalf.

References

1. M. Dragovan, A. A. Stark, R. Pernic, and M. A. Pomerantz, "Millimetric sky-opacity measurements from the South Pole," Appl. Opt. **29,** 463–466 (1990).
2. W. D. Smythe and B. V. Jackson, "Atmospheric water vapor at the South Pole," Appl. Opt. **16,** 2041–2042 (1977).
3. D. E. Hogg, "A summary of the data obtained during the mmA site survey," Millimeter Array Memo 79 (National Radio Astronomy Observatory, Socorro, New Mexico, 1992).
4. Zhong-Yi Liu, *225-GHz Atmospheric Receiver—User's Manual,* Electronics Division Internal Rep. 271 (National Radio Astronomy Observatory, Socorro, New Mexico, 1987).
5. M. McKinnon, *Measurement of Atmospheric Opacity Due to Water Vapor at 225 GHz,* Millimeter Array Memo 40 (National Radio Astronomy Observatory, Socorro, New Mexico, 1987).
6. K. Rohlfs, *Tools of Radio Astronomy* (Springer-Verlag, Berlin, 1986) pp. 166–167.
7. H. J. Liebe, "MPM—an atmospheric millimeter-wave propagation model," Int. J. Infrared Millimeter Waves **10,** 631–650 (1989).